



Influence of temperature and Fe_2O_3 on phosphorus recovery from dephosphorization slag by reduction

Sai He¹ · Lu Lin¹ · Ya-qin Liu¹ · Zhong-xiao Hou¹ · Yan Lv¹ · Wei Wu¹

Received: 22 April 2022 / Revised: 25 May 2022 / Accepted: 13 June 2022 / Published online: 4 February 2023
© China Iron and Steel Research Institute Group Co., Ltd. 2023

Abstract

The reduction and recovery of P_2O_5 in dephosphorization slag were examined to establish a new recycling process for dephosphorization slag. The dephosphorization slag is obtained from the dephosphorization furnace in the duplex converter process, and the content of P_2O_5 in the dephosphorization slag can reach 9 wt.%. The dephosphorization slag is considered to be a prospective resource of phosphorus due to its high content of P_2O_5 . To explore the effects of temperature and Fe_2O_3 content in slag on phosphorus recovery from dephosphorization slag, the experimental slag was reduced by carbon powder in a resistance furnace. The results show that the temperature and content of Fe_2O_3 in slag have a significant effect on the reduction in P_2O_5 , and the reduction and recovery ratios of P_2O_5 in slags increase with the increase in the experimental temperature and content of Fe_2O_3 , reaching 94.41% and 83.09%, respectively. It has been indicated that phosphorus recovery from dephosphorization slag using carbothermic reduction has significant environmental and economic benefits.

Keywords Dephosphorization slag · Phosphorus recovery · Carbothermic reduction · P_2O_5

1 Introduction

Phosphorus is an important nutrient for all organisms on earth, and it is also an essential component in some metallic materials. Study suggested that the world may deplete its abundant phosphorus reserves by around 2300 [1]. This evokes the need for new phosphorus recovery techniques to meet future generations' needs for phosphorus [2, 3]. Many investigations on phosphorus recovery from steelmaking slag due to its high P_2O_5 content have been published [4]. Additionally, the global crude steel output has surpassed 1800 Mt since 2018 [5, 6], and 100–150 kg steelmaking slag is generated when producing a ton of steel in the steelmaking process. Hence, the amount of steelmaking slag is massive. For these reasons, researchers have considered steelmaking slag as a secondary resource for phosphorus and studied its recovery from steelmaking slag [7].

Phosphorus in steelmaking slag is found in the dicalcium silicate phase [8–10]; different additives are used to change the converter slag to increase the solubility of phosphorus in the dicalcium silicate phase [11–19]. After that, the P-rich phase can be separated from the steelmaking slag by a magnetic field [20, 21]. However, the P-rich phase is hard to separate from the steelmaking slag.

Some techniques use the acid leaching method to recover phosphorus from steel slag [22–27], but a large amount of calcium is lost in this process, and it is easy to introduce other environmental problems and expensive treatment costs in the process of acid leaching, which is not conducive to the reuse of slag. Additionally, methods like supergravity have also been reported [28–31], but this process is costly.

The method of reduction by carbonaceous material has also been extensively researched. Shin et al. [32] carried out reduction tests on P_2O_5 in the slag, varying the modified basicity ranging from 0.50 to 1.49. The findings revealed that low basicity contributes to the reduction in P_2O_5 but did not clarify the particular recovery ratios of P_2O_5 in the slag. Nakase et al. [33] researched the effect of the Fe_2O_3 content on the reduction and separation behavior of P_2O_5 in slag and found that 60% of the P_2O_5 was

✉ Lu Lin
linlu_luke@sina.com

¹ Metallurgical Technology Research Institute, Central Iron and Steel Research Institute Co., Ltd., Beijing 100081, China

reduced for slag with $w_{\text{CaO}}/w_{\text{SiO}_2}$ of 1.0 at 1673 K, but there was no P_2O_5 reduced for slag with $w_{\text{CaO}}/w_{\text{SiO}_2}$ of 2.0 at 1673 K, where w_{CaO} and w_{SiO_2} are the mass percent of CaO and SiO_2 in slag, respectively. The findings revealed that the low basicity was conducive to the reduction in P_2O_5 , and the content of Fe_tO had significant impact on the decrease in P_2O_5 in slag. However, this study focused solely on low phosphorus slag ($w_{\text{P}_2\text{O}_5} < 1.6$, where $w_{\text{P}_2\text{O}_5}$ is the mass percent of P_2O_5 in slag). Xue et al. [34] investigated the reduction behavior of P_2O_5 in steelmaking slag in a converter directly using carbonaceous material, and the results showed that more than 70 wt.% of the phosphorus was removed by phosphorus vaporization, and high basicity was not conducive to the recovery of phosphorus in steelmaking slag, but the efficiency of direct reduction by carbonaceous material was very high.

As described above, low basicity and high Fe_tO content are conducive to the recovery of phosphorus in slag. The goal of this research was to recover phosphorus from the dephosphorization slag derived from the dephosphorization furnace (D-P furnace) in the duplex converter process because this type of steelmaking slag has relatively low basicity (about 1.5) and a high content of P_2O_5 (2–9 wt.%). In this study, the effect of temperature and Fe_2O_3 content on the reduction in high-phosphorus dephosphorization slag was researched, the recovery ratio of phosphorus was calculated, and the behavior of phosphorus vaporization was clarified. Results obtained from the present study will provide some references for phosphorus recovery from high-phosphorus dephosphorization slag through reduction.

2 Experimental

2.1 Materials

As shown in Fig. 1, the high-phosphorus dephosphorization slag stated in this work came from a D-P furnace. In the conventional converter process, D-P, D-C (decarbonization), and D-Si (desilication) are conducted in the same furnace. However, in the duplex converter process, D-P and D-Si are first conducted in the D-P furnace [35], while D-C is performed in the D-C furnace; thus, the consumption of lime can be greatly reduced. Therefore, as demonstrated in Table 1, the P_2O_5 content in dephosphorization slag (2–9 wt.%) is higher than that in conventional converter slag (0.5–3 wt.%), and the basicity of dephosphorization slag (about 1.5) is lower than that of the conventional converter slag (about 3.5).

Based on the compositions in Table 1, reagent-grade CaO, Fe_2O_3 , SiO_2 , $\text{Ca}_3(\text{PO}_4)_4$, MnCO_3 , MgO, and Al_2O_3 were used to simulate synthesized slag. Here, Fe_2O_3 was

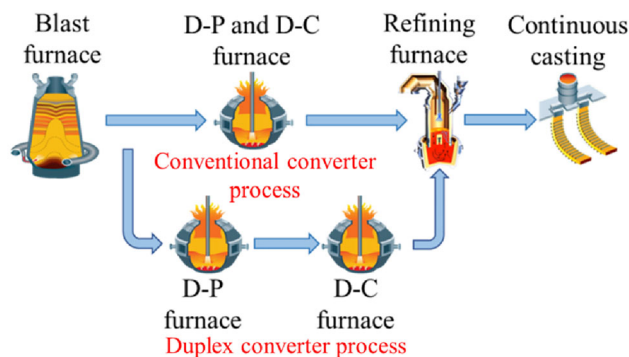


Fig. 1 Schematic diagram of duplex converter process and conventional converter process

used instead of FeO in dephosphorization slag, for Ito et al. [36] found that the distribution behavior of P_2O_5 between solid solution and liquid phase was not different when the iron oxide was changed from FeO to Fe_2O_3 . Fe_2O_3 can be reduced to FeO at temperature above 825 K, and it is considered an FeO state in the experiment. The experimental slags were used for each experiment after crushing them into powder (with a particle size less than 75 μm). The specific compositions of synthetic slag are shown in Table 2. Furthermore, the experimental number and temperature are listed in Table 2. The experimental slags have been used in the experiments without premelting because of the following reasons. (1) Under the conditions of the experimental temperature (1673–1873 K) and the reduction time (3 h), the experimental slag can be completely melted and reacted. (2) Although the phase compositions of the premelted slag and the slag without premelting are inconsistent before melting, they are all in liquid phase and have the same structure as the liquid slag at experimental temperature. At the same time, previous reports showed that a part of Fe_2O_3 is primarily reduced in the solid phase, and $\text{Ca}_3(\text{PO}_4)_2$ and MnO in the slag do not undergo reduction when the temperature is below 1573 K [33, 37]. (3) This study mainly investigates the phosphorus recovery ratio in equilibrium under certain initial slag conditions. The premelted crucibles, such as Al_2O_3 and MgO [32], may change the experimental slag composition. Moreover, in each group of the experiments, only one of the factors is changed, and the other conditions remain the same; thus, the change trend reflected in the final result of the experiment is consistent.

2.2 Experimental apparatus and process

The photograph and the schematic diagram of the experimental apparatus used in the slag reduction studies are shown in Fig. 2. In the experiments, 200 g of the slag

Table 1 Slag compositions of dephosphorization slag from D-P furnace

Chemical composition/wt.%								Basicity (CaO/SiO ₂)
CaO	SiO ₂	MgO	P ₂ O ₅	MnO	FeO	TFe	Al ₂ O ₃	
23–37	14–24	4–6	2–9	9–13	13–34	10–26	1.5–4.0	1.5

Table 2 Chemical compositions of slag for experiments

Experiment No.	Chemical composition/wt.%							Basicity (CaO/SiO ₂)	Temperature/K
	CaO	SiO ₂	MgO	P ₂ O ₅	MnO	Fe ₂ O ₃	Al ₂ O ₃		
1–1	34.20	22.80	5.00	6.00	10.00	20.00	2.00	1.5	1673
1–2	34.20	22.80	5.00	6.00	10.00	20.00	2.00	1.5	1723
1–3	34.20	22.80	5.00	6.00	10.00	20.00	2.00	1.5	1773
1–4	34.20	22.80	5.00	6.00	10.00	20.00	2.00	1.5	1823
1–5	34.20	22.80	5.00	6.00	10.00	20.00	2.00	1.5	1873
2–1	35.66	23.77	5.21	2.00	10.43	20.85	2.09	1.5	1773
2–2	34.93	23.29	5.11	4.00	10.21	20.43	2.04	1.5	1773
2–3	33.47	22.31	4.89	8.00	9.79	19.57	1.96	1.5	1773
2–4	32.74	21.83	4.79	10.00	9.57	19.15	1.91	1.5	1773
3–1	29.58	19.72	4.32	6.00	8.65	30.00	1.73	1.5	1773
3–2	24.96	16.64	3.65	6.00	7.30	40.00	1.46	1.5	1773

sample and a specific amount of carbon powder were charged in a MgO crucible and heated together to the set temperature at the average rate of 10 K/min in a tubular resistance furnace. The carbon powder was used as the reductant in this experiment, and its mass was set 1.5 times the stoichiometric mass necessary to reduce all the Fe₂O₃, P₂O₅, and MnO. The carbon powder was homogeneously mixed with the slag sample. In experiments, the MgO crucible was placed in a graphite crucible and then, they were heated together in a tubular resistance furnace as shown in Fig. 2.

The experimental heating curve is shown in Fig. 3. After the experimental slag was heated to the set temperature defined by the experimental requirements, as shown in Table 2 (1673, 1723, 1773, 1823, and 1873 K), the slag was held at the set temperature for 180 min to guarantee that the slag was entirely melted and the reaction reached equilibrium. The temperature was measured using a thermocouple at the top of the experimental slag. Throughout the experiment process, the flow of Ar gas from the bottom of the tube furnace was 1 L/min to maintain the inert atmosphere in the furnace. After the experiment, the metal droplet and the residual slag were sorted and weighed separately, and then, the experimental slag samples were ground to a particle size of less than 75 μm before the test of chemical composition. The chemical compositions of P, Mn, Fe, Si, and Ca in the slag and metal droplets were analyzed by inductively coupled plasma atomic emission

spectroscopy (ICP-AES, P/Mn (NACIS/CH 008: 2020), Fe (NACIS/CH 143: 2015), Si (NACIS/CH 009: 2013R1), and CaO (NACIS/CH 074: 2013)), and the carbon content in the metal droplet was analyzed using a combustion infrared spectrometer (GB/T 20123–2006). The FeO in the slag was analyzed using the potassium dichromate titrimetric method (GB/T 6730.8–2016).

The mass of the slag was calculated by CaO balance, assuming that the mass of CaO was not reduced after the experiment [32]. The masses of the slag and Fe after the experiment are calculated by Eqs. (1) and (2).

$$W_{\text{slag}} = 200 \times \frac{W_{\text{CaO}}^{\text{Initial}}}{w_{\text{CaO}}} \quad (1)$$

$$W_{\text{Fe}} = W_{\text{Fe}}^{\text{Initial}} - \left(\frac{M_{\text{Fe}}}{M_{\text{FeO}}} \right) \times W_{\text{slag}} \times \frac{w_{\text{FeO}}}{100} \quad (2)$$

where W_{slag} and W_{Fe} indicate the masses of the slag and the metallic iron (MFe) after the experiment, respectively; $W_{\text{CaO}}^{\text{Initial}}$ and $W_{\text{Fe}}^{\text{Initial}}$ indicate the masses of CaO and Fe (element) in the initial experimental slag, respectively; w_{FeO} indicates the mass percent of FeO after the experiment; and M_{FeO} and M_{Fe} indicate the molecular mass of FeO and the atomic mass of Fe, respectively. Based on the above calculations by Eqs. (1) and (2) and the mass fraction of Fe, P, Mn, and Si in metal droplets and slag acquired after the experiment, the distribution of these elements can be obtained.

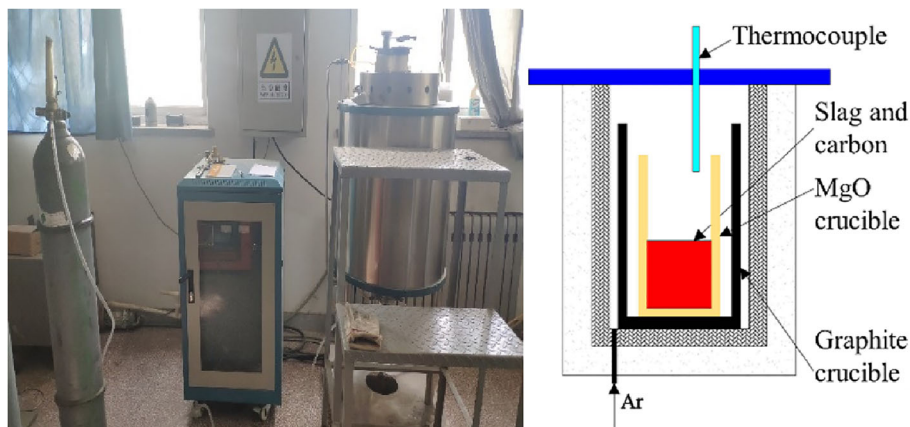


Fig. 2 Photograph of experimental equipment and schematic diagram of resistance furnace

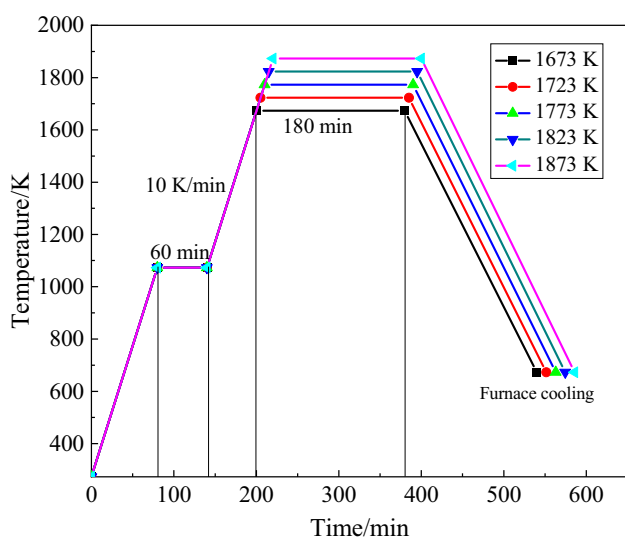


Fig. 3 Heating curves of these experiments

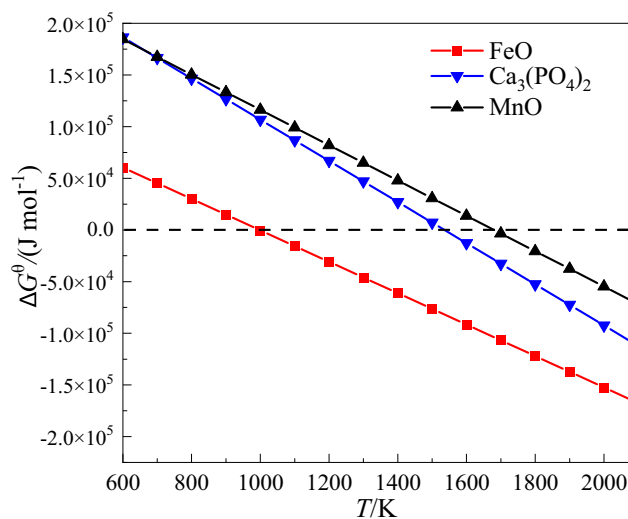


Fig. 4 Relationship between standard Gibbs free energy and temperature

3 Results and discussion

3.1 Thermodynamic analysis of reduction in P_2O_5 , FeO, and MnO

During the reduction process, the FeO, $Ca_3(PO_4)_2$, and MnO in the slag were reduced by carbon powder. The main chemical reactions are shown through Eqs. (3)–(8). And the standard Gibbs free energy of Eqs. (3)–(8) was calculated by FactSage 8.1. These formulas are used to express the trend of the effect of temperature on the reduction reaction.



$$\Delta G_1^0 = 151,686.1 - 152.047T \text{ (J mol}^{-1}\text{)} \quad (4)$$

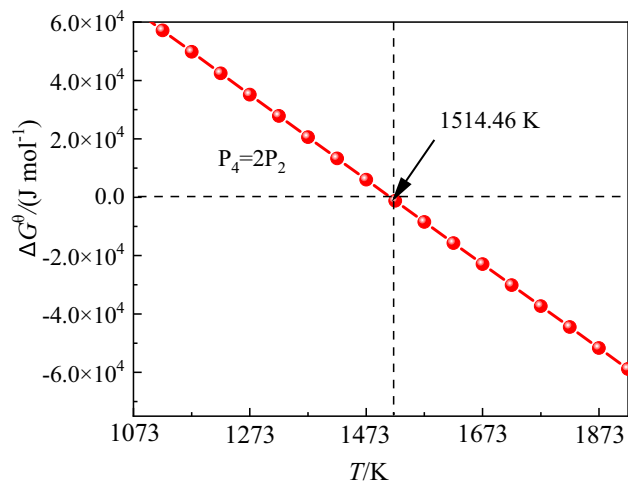


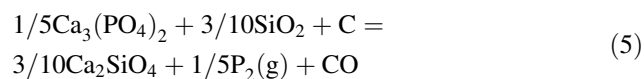
Fig. 5 Standard Gibbs free energy of P_4 formation from P_2 at different temperatures

Table 3 Chemical compositions of slag samples after experiments (wt.%)

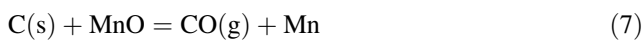
Experiment No.	CaO	SiO ₂	MgO	Al ₂ O ₃	MnO	FeO	P ₂ O ₅
1-1	44.28	29.52	6.47	2.59	10.71	2.26	4.17
1-2	45.05	30.04	6.59	2.63	10.60	1.93	3.17
1-3	45.60	30.40	6.67	2.67	10.62	1.23	2.81
1-4	46.20	30.80	6.75	2.70	10.34	1.06	2.15
1-5	47.57	31.71	6.95	2.78	9.29	0.14	1.56
2-1	46.15	30.76	6.74	2.59	11.43	0.94	1.38
2-2	45.84	30.56	6.71	2.62	10.90	1.19	2.19
2-3	45.79	30.52	6.69	2.74	10.01	1.30	2.95
2-4	45.55	30.37	6.66	2.78	9.13	1.18	4.32
3-1	49.73	28.68	7.26	2.91	9.49	0.90	1.02
3-2	53.06	25.81	7.76	3.10	9.28	0.27	0.71

Table 4 Chemical compositions of metal samples after experiments (wt.%)

Experiment No.	C	Mn	P	Fe	Si
1-1	0.50	1.11	6.22	92.18	< 0.1
1-2	0.69	2.82	7.78	88.65	< 0.1
1-3	0.64	3.30	8.01	86.86	< 0.1
1-4	0.87	6.02	9.03	82.92	< 0.1
1-5	0.84	7.99	9.54	80.08	< 0.1
2-1	0.87	1.71	2.02	94.83	< 0.1
2-2	0.91	2.30	4.92	91.02	< 0.1
2-3	0.47	4.56	10.49	82.44	< 0.1
2-4	0.31	5.77	11.9	77.76	< 0.1
3-1	1.01	4.99	7.92	85.11	< 0.1
3-2	0.91	3.81	6.82	87.41	< 0.1



$$\Delta G_2^0 = 305,831.5 - 199.1T \text{ (J mol}^{-1}\text{)} \quad (6)$$



$$\Delta G_3^0 = 287,214.6 - 170.971T \text{ (J mol}^{-1}\text{)} \quad (8)$$

where ΔG_i^0 is the standard Gibbs free energy of reaction i ; and T is temperature.

As shown in Fig. 4, the initial temperature to reduce FeO, Ca₃(PO₄)₂, and MnO is 997.6, 1536.1, and 1679.9 K, respectively. Thus, FeO, Ca₃(PO₄)₂, and MnO can be reduced at experimental temperature. At the same time, the Gibbs free energy drops as the experimental temperature increases, which means that the higher experimental temperature helps to improve the reduction ratios of Fe₂O₃, P₂O₅, and MnO in the experimental slag.

As we know, the main products of P₂O₅ reduction in the slag are P₂ and P₄ [33], and the relationship between P₂ and P₄ is shown in Fig. 5. Here, thermodynamic calculations were performed by FactSage 8.1.

As shown in Fig. 5, when the temperature is higher than 1514.46 K, the main reduction product is P₂. Figure 5 shows that higher temperature is favorable for P₂ formation, and the main form of phosphorus vaporization was P₂ in this study, theoretically.

3.2 Mass balance before and after experiments

As illustrated in Fig. 6, the samples were divided into metal droplet and slag, and then, the compositions of these two substances were tested. After the experiments, the separation of the metal droplet and slag was complete. For the experimental temperature was higher than 1673 K, and

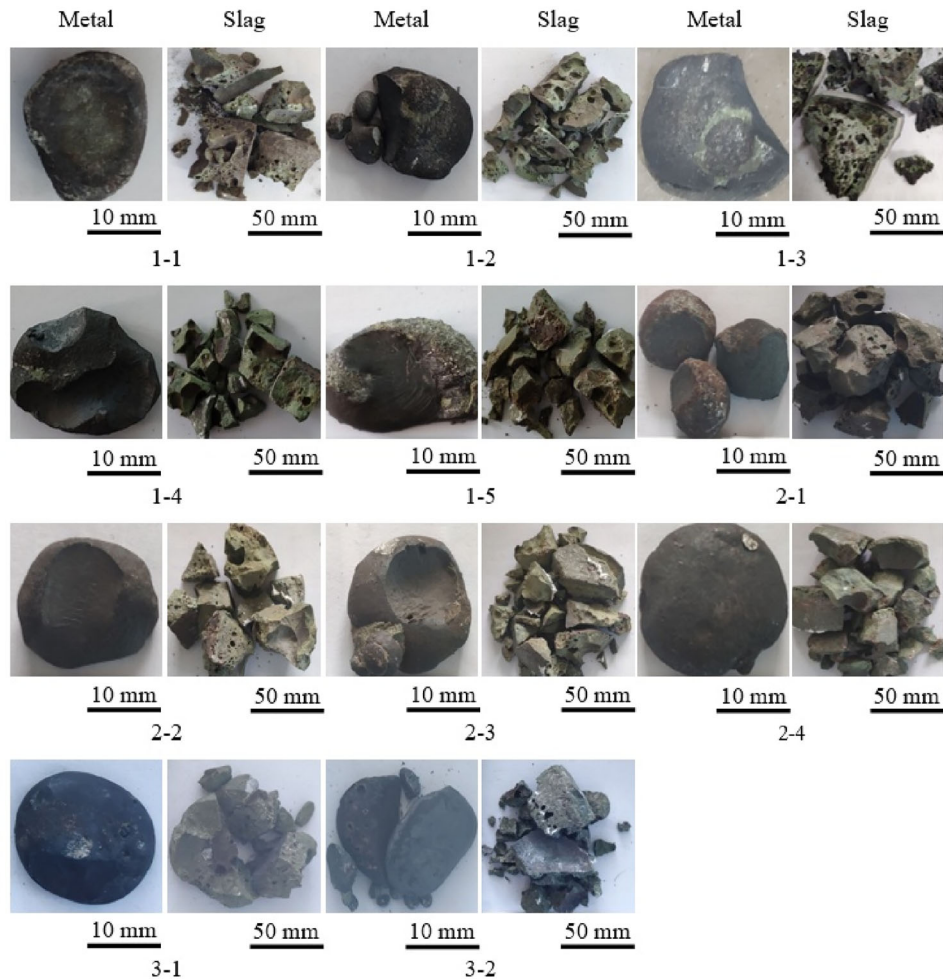


Fig. 6 Images of slag and metal after reduction experiments

the Fe_2O_3 in the initial slag was easily reduced to FeO , the Fe_2O_3 in the reduced slag samples was recognized as FeO .

The chemical compositions of the slag and metal samples are indicated in Tables 3 and 4, respectively. The concentration of Si in metal droplets was less than 0.1 wt.%, and SiO_2 was not considered to be reduced in the experimental slag.

In Experiments (1–1)–(1–5), as the experimental temperature increases, the results show that the content of P_2O_5 in the reduced slag decreases from 4.17 to 1.56 wt.%. High temperature promotes the reduction in P_2O_5 in slag. In Experiments (2–1)–(2–4) and (1–3), as the content of P_2O_5 in the initial experimental slag increases, the content of P_2O_5 in the reduced slag increases from 1.38 to 4.32 wt.%. In Experiments (3–1)–(3–2) and (1–3), as the proportion of Fe_2O_3 in the initial experimental slag grows, the content of P_2O_5 in the reduced slag drops from 2.81 to 0.71 wt.%. The findings show that Fe_2O_3 enhances the reduction in P_2O_5 in slag.

The mass balance of phosphorus in each of the experiments is shown in Fig. 7. To make the comparisons evident, the data from Experiment (1–3) are utilized thrice in Fig. 7.

In Experiments (1–1)–(1–5), as the experimental temperature increases, the phosphorus vaporization ratios increase from 13.79 to 18.03 wt.%, and the recovery ratios increase from 32.57 to 63.31 wt.%. The results reveal that while the experimental temperature has little effect on phosphorus vaporization, and it has a significant impact on phosphorus recovery from slag. The findings suggest that a higher temperature is favorable for dissolving phosphorus in molten iron.

In Experiments (2–1)–(2–4), as the content of P_2O_5 in the initial experimental slag increases, the phosphorus vaporization ratios increase from 12.55 to 24.26 wt.%, and the recovery ratios increase from 29.59 to 32.77 wt.%. The results show that under the assumption that other compositions in slag remain unchanged, and the increase in P_2O_5 content in slag promotes the vaporization of phosphorus.

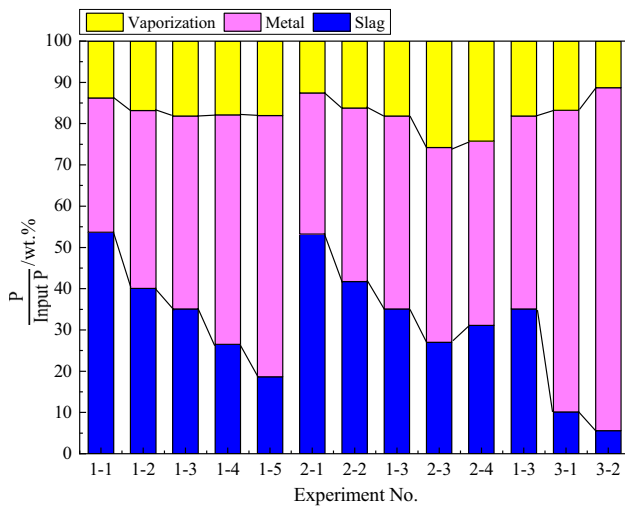


Fig. 7 Mass balance of P after experiments

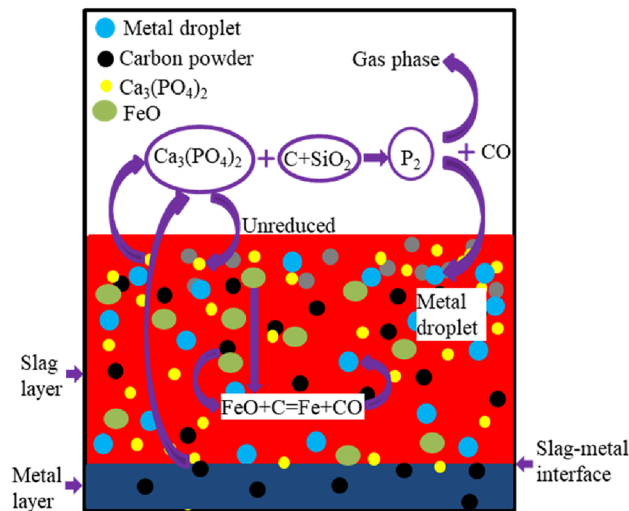


Fig. 8 Schematic diagram of reaction and whereabouts of phosphorus and iron

In Experiments (3–1), (3–2), and (1–3), as the content of Fe₂O₃ in the initial experimental slag increases, the recovery ratios of P₂O₅ increase from 46.75 to 83.09 wt.%, and the vaporization ratios fall from 18.14 to 11.32 wt.%. The findings demonstrate that the great content of Fe₂O₃ in the slag increases phosphorus recovery from the slag substantially.

3.3 Influences of Fe₂O₃ content on reduction and recovery of phosphorus in slag

Most of phosphorus is found in the form of tricalcium phosphate Ca₃(PO₄)₂ in slag [38–40]. As shown in Fig. 8, during the process of the reduction experiment, some of the reduced phosphorus vapor (P₂) contacted metal droplets

and was absorbed in the metal droplet. There was still some Ca₃(PO₄)₂ in the slag that was not reduced, and it ended up in the residual slag. The other part of the reduced phosphorus was not absorbed by the metal droplet, and it was ejected into the gas phase in the form of phosphorus vaporization.

In Experiments (1–3), (3–1), and (3–2), the recovery ratios of phosphorus increased significantly as shown in Fig. 7. With the increase in Fe₂O₃ content in the experimental slag, the number of metal droplets in the slag was increased, which increased the chance of contact between phosphorus vapor and metal droplets. Furthermore, the liquidus temperature of the slag is decreased with the increased content of FeO in the slag as shown in Fig. 9. And the higher content of FeO in slag was better conditioned for the contact of phosphorus vapor (P₂) and liquid metal droplets, and the recovery ratio of phosphorus in the slag was increased.

3.4 Relationship between phosphorus distribution ratio and phosphorus recovery ratio after experiments

The phosphorus distribution ratio L_P is expressed in Eq. (9), and the recovery ratio of P₂O₅ denoted by the parameter $R_{P_2O_5}$ is expressed in Eq. (10),

$$L_P = \frac{w_{(P)}}{w_{[P]}} \tag{9}$$

$$R_{P_2O_5} = \frac{M_{P \text{ in Metal}}}{M_{\text{input P}}} \times 100\% \tag{10}$$

where $w_{(P)}$ means the mass fraction of phosphorus in slag; $w_{[P]}$ means the mass fraction of phosphorus in metal; $M_{P \text{ in Metal}}$ indicates the mass of phosphorus in metal droplets; and $M_{\text{input P}}$ indicates the mass of phosphorus in the initial experimental slag. The calculation of theoretical phosphorus distribution ratio is difficult because the reaction between slag and metal and the compositions of slag are complex [41, 42]. According to previous research results, empirical equations [43–46] for calculating L_P are summarized in Table 5.

Based on the experimental results in Tables 3 and 4, the experimental values of $\lg L_P$ are obtained and shown in Table 6.

As shown in Fig. 10a, $\lg L_P$ has a downward trend with the increasing experimental temperature. Moreover, the experimental values of $\lg L_P$ have similar trends to the values calculated by different empirical equations. As shown in Fig. 10b, $\lg L_P$ has a downward trend with the increasing content of Fe₂O₃ in the experimental slag. In Fig. 10c, $\lg L_P$ has a downward trend with the increasing content of P₂O₅ in experimental slag when the content of

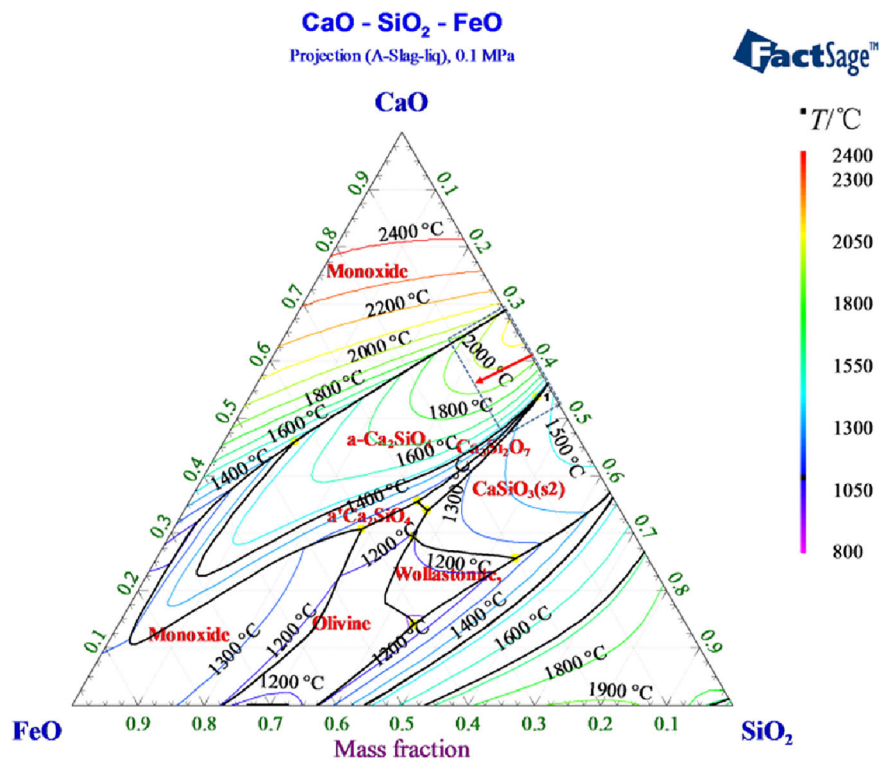


Fig. 9 Polythermal liquidus projection diagram of CaO–SiO₂–FeO system

Table 5 Empirical equations for calculating L_P value

$\lg L_P = 22,350/T - 16 + 0.08w_{\text{CaO}} + 2.5\lg(w_{\text{TFe}})$	(11)
$\lg L_P = -12.24 + 20,000/T + 2.5\lg(w_{\text{FeO}}) + 6.65\lg(w_{\text{CaO}} + 0.8w_{\text{MgO}})/(w_{\text{SiO}_2} + w_{\text{Al}_2\text{O}_3} + 0.8w_{\text{P}_2\text{O}_5})$	(12)
$\lg L_P = 0.072(w_{\text{CaO}} + 0.3w_{\text{MgO}} + 0.6w_{\text{P}_2\text{O}_5} + 0.6w_{\text{MnO}}) + 2.5\lg(w_{\text{TFe}}) + 11,570/T - 10.52$	(13)
$\lg L_P = 2.5\lg(w_{\text{TFe}}) + 0.0715(w_{\text{CaO}} + 0.25w_{\text{MgO}}) + 7710/T - 8.55 + (105.1/T + 0.0723)w_{[\text{C}]}$	(14)
$\lg L_P = 0.072(w_{\text{CaO}} + 0.15w_{\text{MgO}} + 0.6w_{\text{P}_2\text{O}_5} + 0.6w_{\text{MnO}}) + 2.5\lg(w_{\text{TFe}}) + 11,570/T - 10.52$	(15)

P₂O₅ is below 8 wt.%, and then, $\lg L_P$ increases with the increase in P₂O₅ content.

According to the above analysis of $\lg L_P$, the value of $\lg L_P$ is a constant value under a given situation. This indicates that the slag composition (Fe₂O₃ and P₂O₅ contents) and the temperature significantly affect the recovery ratios of phosphorus resources in the slag, although it is difficult to distinguish one factor from the others. $R_{\text{P}_2\text{O}_5}$ can be reflected by the phosphorus content in the slag and the phosphorus content in the metal. Here, the phosphorus distribution ratio L_P , which is a function of the three factors as shown in Eqs. (11)–(15), is introduced as an important index to analyze the phosphorus recovery ratio.

The variations of $R_{\text{P}_2\text{O}_5}$ and $\lg L_P$ are shown in Fig. 11. As shown in Fig. 11, it is clear that there is a negative

correlation between $\lg L_P$ and $R_{\text{P}_2\text{O}_5}$ after the reduction experiment.

According to the experimental results of Experiments (1–1)–(1–5), the value of $\lg L_P$ decreased from –0.53 to –1.15, and the recovery ratio of P₂O₅ increased from 32.57 to 63.31 wt.%.

In Experiments (2–1), (2–2), (1–3), and (2–3), the $\lg L_P$ value decreases from –0.53 to –0.91, and the recovery ratios of P₂O₅ increase from 34.22 to 47.21 wt.%. Furthermore, in Experiments (2–3)–(2–4), the $\lg L_P$ value increases from –0.91 to –0.80, and the recovery ratios of P₂O₅ decrease from 47.21 to 44.66 wt.%.

In Experiments (1–3), (3–1), and (3–2), with the increase in Fe₂O₃ content in slag, the $\lg L_P$ value decreases from –0.80 to –1.34, and the recovery ratios of P₂O₅ increase from 46.75 to 83.09 wt.%.

Table 6 Experimental values of lgL_P

Experiment No.	1-1	1-2	1-3	1-4	1-5	2-1	2-2	2-3	2-4	3-1	3-2
lgL _P	- 0.53	- 0.75	- 0.81	- 0.98	- 1.15	- 0.53	- 0.71	- 0.91	- 0.80	- 1.25	- 1.34

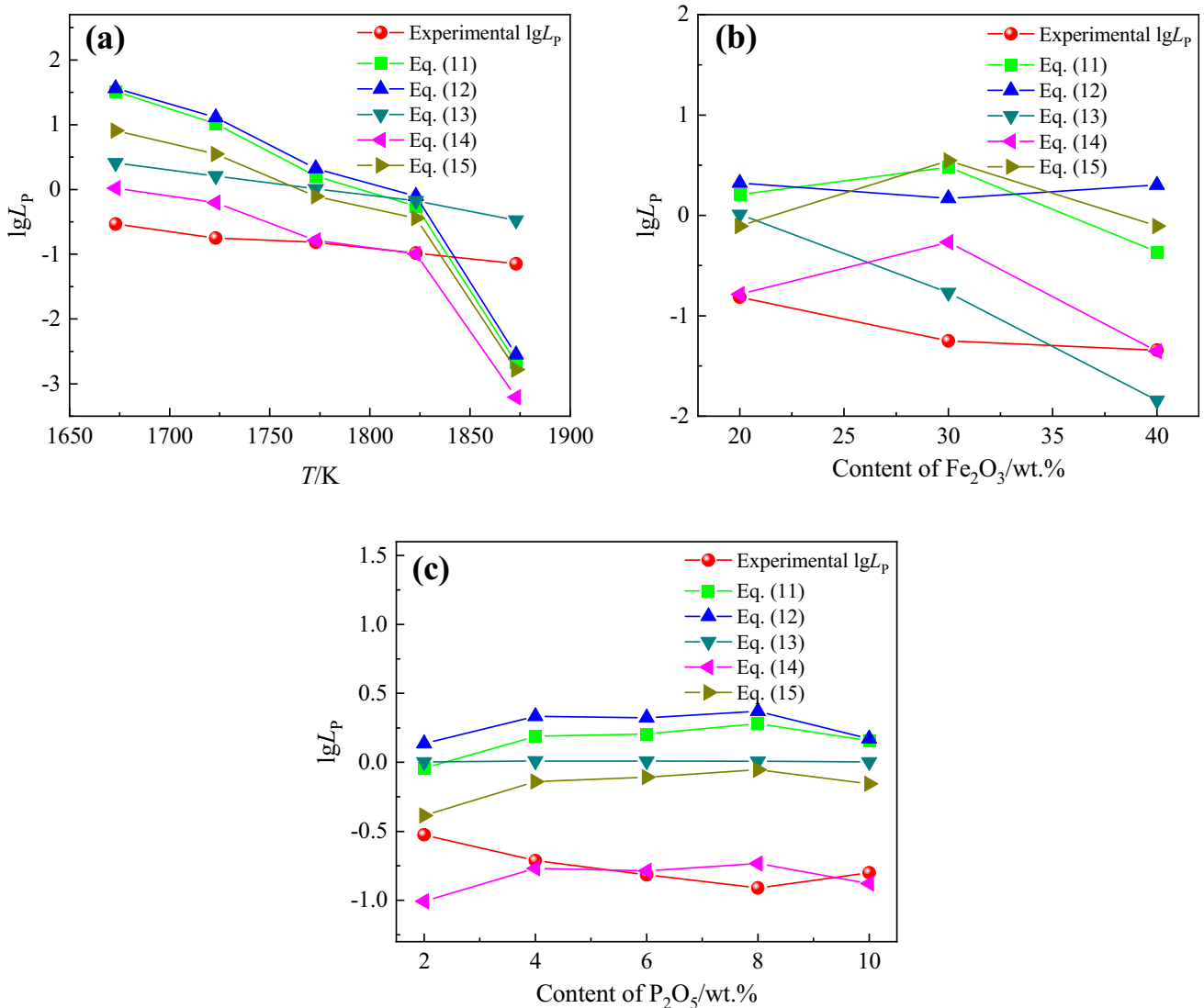


Fig. 10 Comparison of lgL_P between experimental and calculated results at various temperature (a), content of Fe₂O₃ (b), and content of P₂O₅ (c)

According to the above experimental results, it can be seen that the lgL_P value can reflect the recovery ratios of P₂O₅ well after the experiments. It can be concluded from Fig. 11 that the R_{P₂O₅} decreased with the increase in lgL_P.

The relationship in Fig. 11 is converted into the relationship between lgL_P and R_{P₂O₅}, as shown in Fig. 12. After the carbothermic reduction experiments, there was a good linear relationship between R_{P₂O₅} and lgL_P in the experimental results. The relationship is shown in Eq. (16).

$$R_{P_2O_5} = 0.17 - 57.65lgL_P \tag{16}$$

The results showed that R_{P₂O₅} can be calculated by lgL_P after the experiments. Through Eq. (16), it can be seen that when lgL_P is below - 1, R_{P₂O₅} can exceed 57%.

R_{P₂O₅} can be calculated by the final phosphorus content in slag and the phosphorus content in metal droplets. At the same time, as shown in Fig. 8, the experimental values of lgL_P have similar trends calculated by Eqs. (11)–(15). The

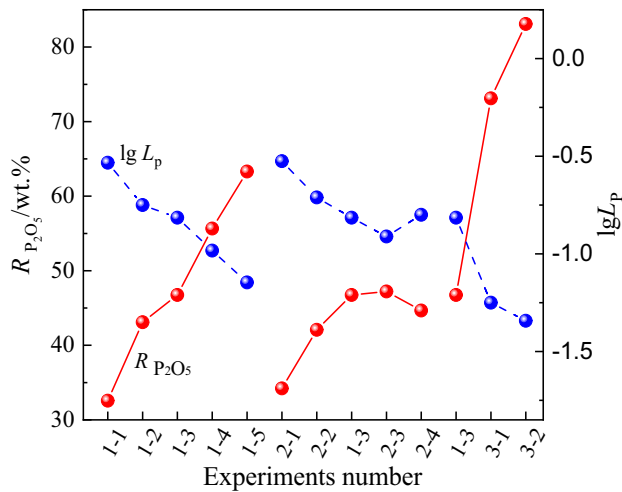


Fig. 11 Relationship between $R_{P_2O_5}$ and $\lg L_P$

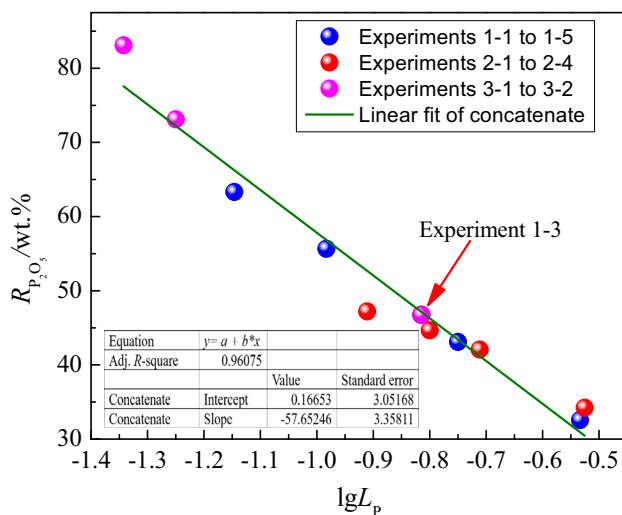


Fig. 12 Relationship between $\lg L_P$ and recovery ratio of P_2O_5 after experiments

trend of $R_{P_2O_5}$ can also be estimated by $\lg L_P$ which is obtained by the empirical equations as shown in Table 5. It was proved that $R_{P_2O_5}$ was mainly affected by the contents of CaO and FeO as shown in Eqs. (11)–(15). According to Eqs. (11)–(15), it can be seen that MgO, Al_2O_3 , and MnO may have a certain effect on the value of $\lg L_P$, but there is no experimental research and analysis in the present study.

4 Conclusions

1. Higher temperature aided in the reduction and recovery of P_2O_5 in slag. At 1873 K, 81.34 wt.% of P_2O_5 in the slag is reduced, and 77.83 wt.% of the reduced P_2O_5 is recovered by metal droplets.

2. With the increase in P_2O_5 content from 2 to 10 wt.% in the initial experimental slag, the content of P in the metal droplet increased from 2.02 to 11.90 wt.%, and the vaporization ratios of P_2O_5 increased as the P_2O_5 content increased in experimental slag.
3. When the Fe_2O_3 content is increased in the initial slag, it is conducive to the recovery of P_2O_5 in slag during the reduction process. When the content of Fe_2O_3 is increased from 20 to 40 wt.%, the reduction ratios of P_2O_5 increased from 64.89 to 94.41 wt.%, and the recovery ratios of the reduced P_2O_5 increased from 72.05 to 88.01 wt.%.
4. The recovery ratio of P_2O_5 can be reflected by the value of phosphorus distribution ratio. The relationship between them can be expressed by the following formula $R_{P_2O_5} = 0.17 - 57.65 \lg L_P$.

Acknowledgements The research was financially sponsored by the National Natural Science Foundation of China (Grant Nos. 51704080, 51874102 and 52074093) and the National Key Research and Development Program of China (Grant No. 2019YFC1905200).

Declarations

Conflict of interest The authors declare no conflict of interest.

References

- [1] S. Daneshgar, A. Callegari, A.G. Capodaglio, D. Vaccari, Resources 7 (2018) 37.
- [2] M.C. Tomei, V. Stazi, S. Daneshgar, A.G. Capodaglio, Sustainability 12 (2020) 575.
- [3] S. Daneshgar, A. Buttafava, A. Callegari, A.G. Capodaglio, J. Clean. Prod. 223 (2019) 729–738.
- [4] C.M. Du, X. Gao, S. Ueda, S.Y. Kitamura, ISIJ Int. 58 (2018) 860–868.
- [5] K. He, L. Wang, X. Li, Metals 10 (2020) 302.
- [6] World Steel Association, World steel in figures 2018–2021. <https://worldsteel.org/steel-by-topic/statistics/world-steel-in-figures/>.
- [7] Y. Li, W.B. Dai, J. Clean. Prod. 175 (2018) 176–189.
- [8] L. Lin, Y.P. Bao, C. Gu, W. Wu, J.Q. Zeng, High Temp. Mater. Proc. 37 (2018) 655–663.
- [9] X.R. Wu, P. Wang, L.S. Li, Z.J. Wu, R.H. Chen, Ironmak. Steelmak. 38 (2011) 185–188.
- [10] J.Y. Li, M. Zhang, M. Guo, X.M. Yang, Metall. Mater. Trans. B 45 (2014) 1666–1682.
- [11] C. Su, N.N. Lv, J.X. Yang, L.S. Wu, H.C. Wang, Y.C. Dong, J. Iron Steel Res. Int. 26 (2019) 42–51.
- [12] C.M. Du, N.N. Lv, C. Su, W.M. Liu, J.X. Yang, H.C. Wang, J. Iron Steel Res. Int. 26 (2019) 1162–1170.
- [13] L. Lin, Y.P. Bao, M. Wang, H.M. Zhou, L.Q. Zhang, Ironmak. Steelmak. 40 (2013) 521–527.
- [14] L. Lin, Y.P. Bao, M. Wang, W. Jiang, H.M. Zhou, ISIJ Int. 54 (2014) 2746–2753.
- [15] L. Lin, Y.P. Bao, W. Jiang, Q.F. Wu, ISIJ Int. 55 (2015) 552–558.

- [16] L. Guo, J.T. Gao, S.P. Zhong, Z.C. Guo, *J. Iron Steel Res. Int.* 26 (2019) 113–122.
- [17] D. Makhija, R.K. Rath, K. Chakravarty, A.S. Patra, A.K. Mukherjee, A.K. Dubey, *Int. J. Miner. Metall. Mater.* 23 (2016) 751–759.
- [18] H. Suito, R. Inoue, *Trans. Iron Steel Inst. Jpn.* 24 (1984) 47–53.
- [19] Z. Yan-Ling, G. Ming, L. Feng-Shan, Y. Kan, *Arch. Metall. Mater.* 63 (2018) 1769–1783.
- [20] K. Yokoyama, H. Kubo, K. Mori, H. Okada, S. Takeuchi, T. Nagasaka, *ISIJ Int.* 47 (2007) 1541–1548.
- [21] H. Kubo, K. Matsubae-Yokoyama, T. Nagasaka, *ISIJ Int.* 50 (2010) 59–64.
- [22] S. Sugiyama, I. Shinomiya, R. Kitora, K. Nakagawa, M. Katoh, *J. Chem. Eng. Jpn.* 47 (2014) 483–487.
- [23] J. Diao, L. Jiang, Y.H. Wang, B. Xie, Phosphorus, Sulfur, and Silicon and the Related Elements 190 (2015) 387–395.
- [24] M. Numata, N. Maruoka N, S.J. Kim, S.Y. Kitamura, *ISIJ Int.* 54 (2014) 1983–1990.
- [25] T. Teratoko, N. Maruoka, H. Shibata, S.Y. Kitamura, *High Temp. Mater. Proc.* 31 (2012) 329–338.
- [26] J. Diao, Z. Ke, L. Jiang, T. Zhang, B. Xie, *Miner. Process. Extract. Metall.* 125 (2016) 103–108.
- [27] L. Lin, Y.P. Bao, M. Wang, W. Jiang, H.M. Zhou, *J. Iron Steel Res. Int.* 21 (2014) 496–502.
- [28] T. Iwama, C.M. Du, S. Koizumi, X. Gao, S. Ueda, S.Y. Kitamura, *Tetsu-to-Hagané* 105 (2019) 479–487.
- [29] C. Li, J.T. Gao, F.Q. Wang, Z.C. Guo, *Ironmak. Steelmak.* 45 (2018) 44–49.
- [30] C. Li, J.T. Gao, Z.C. Guo, *ISIJ Int.* 56 (2016) 759–764.
- [31] C. Li, J.T. Gao, Z.C. Guo, *Metall. Mater. Trans. B* 47 (2016) 1516–1519.
- [32] D.J. Shin, X. Gao, S. Ueda, S.Y. Kitamura, *Metall. Mater. Trans. B* 50 (2019) 1248–1259.
- [33] K. Nakase, A. Matsui, N. Kikuchi, Y. Miki, *ISIJ Int.* 57 (2017) 1197–1204.
- [34] Y.K. Xue, D.G. Zhao, S.H. Wang, C.X. Li, R.H. Guo, *Ironmak. Steelmak.* 47 (2020) 892–898.
- [35] X.F. Bai, Y.H. Sun, L. Luo, C.L. Zhao, *J. Iron Steel Res. Int.* 27 (2020) 148–159.
- [36] K. Ito, M. Yanagisawa, N. Sano, *Tetsu-to-Hagané* 68 (1982) 342–344.
- [37] Y.Y. Zhang, Fundamental research on iron and phosphorus separation of high-phosphorus iron ore by direct reduction, University of Science and Technology Beijing, Beijing, China, 2018.
- [38] S. Kitamura, H. Shibata, K. Shimauchi, S. Saito, *Metall. Res. Technol.* 105 (2008) 263–271.
- [39] S.L. Xie, W.L. Wang, *Steel Res. Int.* 87 (2016) 376–385.
- [40] K. Matsubae-Yokoyama, H. Kubo, T. Nagasaka, *ISIJ Int.* 50 (2010) 65–70.
- [41] G.F. Ye, J. Yang, R.H. Zhang, W.K. Yang, H. Sun, *Int. J. Miner. Metall. Mater.* 28 (2021) 66–75.
- [42] C.M. Lee, R.J. Fruehan, *Ironmak. Steelmak.* 32 (2005) 503–508.
- [43] G.W. Healy, *J. Iron Steel Inst.* 208 (1970) 664–668.
- [44] H. Suito, R. Inoue, *Trans. Iron Steel Inst. Jpn.* 24 (1984) 40–46.
- [45] K. Ide, R.J. Fruehan, *Iron Steelmak.* 27 (2000) 65–70.
- [46] Y. Ogawa, M. Yano, S.Y. Kitamura, H. Hirata, *Steel Res. Int.* 74 (2003) 70–76.

Springer Nature or its licensor (e.g. a society or other partner) holds exclusive rights to this article under a publishing agreement with the author(s) or other rightsholder(s); author self-archiving of the accepted manuscript version of this article is solely governed by the terms of such publishing agreement and applicable law.